

Figure 2. Transient absorbance monitored at 390 (upper trace) and 460 nm (lower trace) for 5×10^{-3} M TI/1.0 M TEA in benzene, 532-nm laser excitation.

time scale.¹⁹ Time-resolved difference spectra resulting from 532-nm laser excitation of degassed solutions of TI with 1.0 M TEA in benzene show immediately after the laser pulse (10–20 ns) a broad absorbance that extends from 360 to 500 nm. After 500 ns the difference spectrum evolves to a more resolved absorbance centered at 390 nm extending to 450 nm. This spectrum persists out to the maximum time delays obtainable (50–100 μ s); notable is the fact that this spectrum is similar to that of TIH_2 (see Figure 1). Time evolution of the absorbance at 390 and 460 nm is shown in Figure 2. At 460 nm a transient absorbance is noted; the transient decays to 20% of the initial value with a first-order rate constant $k = 3.6 \times 10^6 \text{ s}^{-1}$ ($\tau = 280 \text{ ns}$) and remains constant out to long times. At 390 nm an initial step is noted with the laser pulse followed by a grow in concurrent with the above decay. We attribute the 460-nm transient to the species $\text{TIH}\cdot$ as first a radical pair [$\text{TIH}\cdot, \cdot\text{D}$] and subsequently the free radical. The 390-nm absorbance appears due to both $\text{TIH}\cdot$ and TIH_2 , but primarily to the latter at long times.

The laser flash experiments suggest that two pathways exist for formation of TIH_2 from the radical pair formed via pho-

toinduced electron transfer–proton transfer. These paths are outlined in Scheme I. The residual absorbance at 460 nm can be attributed to free radicals, $\text{TIH}\cdot$, that form TIH_2 via disproportionation. The presence of this path is supported by ESR studies which confirm the generation of a single radical with a hyperfine spectrum attributable to $\text{TIH}\cdot$.^{21,22} However the bulk of the product formed in benzene is generated too rapidly to occur via this second-order process. The relatively rapid reaction of $\text{TIH}\cdot$ from the radical pair that competes with free radical formation is evidently a second electron transfer occurring within the radical pair (hence first order with $k = 3 \times 10^6 \text{ s}^{-1}$), as outlined in Scheme I. This path provides a two-electron reduction or net *hydride transfer* from the tertiary amine to TI before the radicals diffuse apart.²²

While the present reaction is noteworthy in that it involves a single photon initiated net two electron transfer, it should be anticipated to be possible or even general for a variety of appropriately matched donors and acceptors where an intervening proton transfer can occur. The long lifetime for the radical pair in the present case (or relatively slow rate for the second electron transfer) suggests that the pair should be a triplet and that intersystem crossing has occurred subsequent to or concurrent with the electron-transfer quenching.²³ It is reasonable to anticipate that the lifetime of the radical pair and relative importance of the paths in Scheme I should vary with solvent polarity and viscosity. We are currently examining this for the above and a number of related reactions.

Acknowledgment. We are grateful to the U. S. Department of Energy (Contract DE-AS05-81ER10815.A000) for support of this research.

Registry No. Thioindigo, 522-75-8; *N*-benzyl-1,4-dihydrocinotinamide, 952-92-1; *N*-methylacridan, 4217-54-3.

(21) Solutions of TI with tertiary amines, hydroquinone, and phenol during photolysis show a single ESR signal (5 line, $g_{\text{iso}} = 2.0040 \pm 0.0001$, $a_{\text{N}} = 15.40 \pm 0.01 \text{ G}$) attributed to $\text{TIH}\cdot$.

(22) Studies suggest that CH_3CNEt_2 has sufficient potential to reduce TI and $\text{TIH}\cdot$.¹²

(23) Further experiments (e.g., CIDNP) to provide evidence that the radical pair is indeed a triplet are planned. Alternatively, the stability of $\text{TIH}\cdot$ may account for the radical pair lifetime.

Two Novel Examples of Hydroxylation of Aromatic Rings in Coordination Chemistry

Pinaki Bandyopadhyay,^{1a} Debkumar Bandyopadhyay,^{1a}
Animesh Chakravorty,^{*1a} F. Albert Cotton,^{*1b}
Larry R. Falvello,^{1b} and Scott Han^{1b}

Department of Inorganic Chemistry
Indian Association for the Cultivation of Science
Calcutta 700032, India
Department of Chemistry
and Laboratory for Molecular Structure and Bonding
Texas A&M University
College Station, Texas 77843

Received June 3, 1983

The hydroxylation of an aromatic ring, i.e., $\text{ArH} \rightarrow \text{ArOH}$, is an important process in chemistry and biology.² We report here two novel examples of this reaction, each occurring in a coordination complex in which the aryl group is part of an arylazo

(19) Laser flash photolysis apparatus as described in ref 20, except a pulsed monitoring lamp was used.

(20) Winkle, J. R.; Worsham, P. R.; Schanze, K. S.; Whitten, D. G. *J. Am. Chem. Soc.*, in press.

(1) (a) Indian Association for the Cultivation of Science. (b) Texas A&M University.

(2) Hayaishi, O., Ed., "Molecular Mechanisms of Oxygen Activation"; Academic Press: New York, 1974.

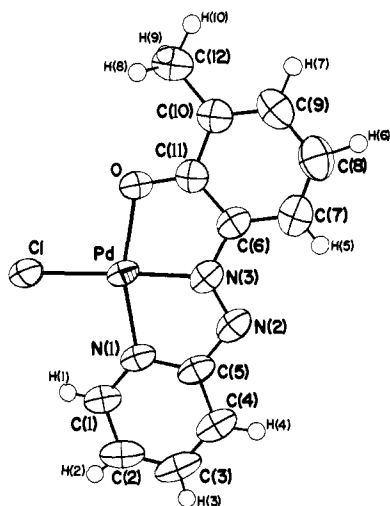
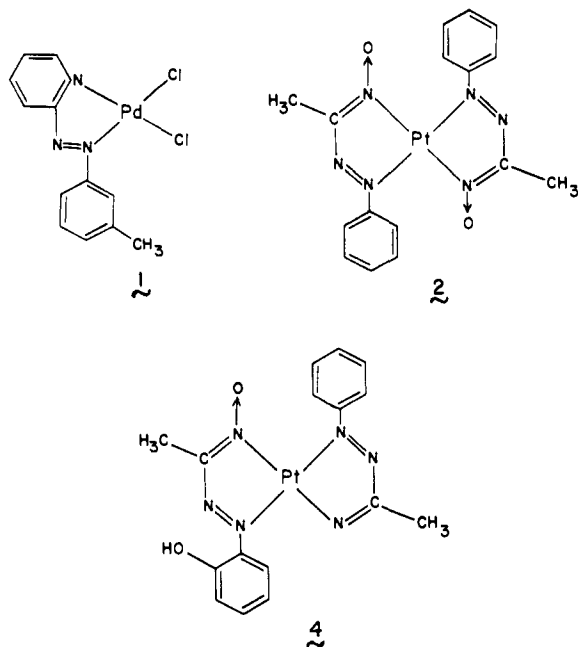


Figure 1. Molecular structure of compound **3**. Some important bond lengths and angles: Pd–Cl, 2.291 (2); Pd–O, 2.044 (3); Pd–N(1), 2.012 (4); Pd–N(3), 1.925 (4); O–C(11), 1.302 (6); N(2)–N(3), 1.282 (5) Å; Cl–Pd–O, 100.1 (1)°; Cl–Pd–N(1), 97.9 (1)°; Cl–Pd–N(3), 177.2 (1)°; O–Pd–N(1), 161.9 (2)°; O–Pd–N(3), 82.7 (2)°; N(1)–Pd–N(3), 79.3 (2)°.

function. The parent complexes are dichloro(2-*m*-tolylazopyridine)palladium(II) (**1**) and *trans*-bis(phenylazoacetal-



doximato)platinum(II) (**2**). While the structure of **2** is accurately known from X-ray work,³ that of **1** is inferred from infrared and other data.^{4,5,20}

On boiling the yellow suspension of **1** in water⁶ in the presence⁷

(3) Bandyopadhyay, D.; Bandyopadhyay, P.; Chakravorty, A.; Cotton, F. A.; Falvello, L. R. *Inorg. Chem.* **1983**, *22*, 1315.

(4) The binding mode of the azopyridine ligand shown in **1** is well-documented in ruthenium(II) complexes⁵ of this ligand. The cis PdCl₂ group in **1** has characteristic stretches at 360 and 345 cm⁻¹. Anal. Calcd for PdC₁₂H₁₁N₃Cl₂: C, 38.48; H, 2.96; N, 11.22. Found: C, 38.18; H, 3.07; N, 11.13.

(5) Goswami, S.; Chakravarty, A. R.; Chakravorty, A. *Inorg. Chem.* **1983**, *22*, 602.

(6) The original purpose of this experiment was to prepare and study the diaquo analogue (chloride replaced by H₂O) of **1**. This has never been accomplished even under mild reaction conditions; complex **3** results instead. In this respect the behavior of **1** is entirely different from that of its ruthenium(II) analogue,⁵ which undergoes facile aquation in the presence of Ag⁺ and hydroxylation of the aromatic ring does not occur. The hydroxylation reaction is specific for the palladium complex.

of dissolved Ag⁺, a dark colored solid is deposited. On purification⁸ this solid yields a crystalline green complex of composition PdC₁₂H₁₀N₃OCl (**3**) in 20% yield. The deep green dichloromethane solution has an electronic band at 680 nm ($\epsilon \sim 6000$) with shoulders at 640 and 740 nm. The structure of complex **3** as determined X-ray crystallographically⁹ is shown in Figure 1. The molecule is essentially planar with no atom deviating >0.08 Å from the best plane. The phenyl ring has undergone hydroxylation¹⁰ with subsequent formation of a Pd–O bond. The C–O bond distance (1.302 (6) Å) is indicative of considerable double-bond character. The good π -acceptor character of the azo group⁵ is evidenced by the shortness of the Pd–N(3) bond, 1.925 (4) Å, compared to the Pd–N(1) bond, 2.012 (4) Å.

When a suspension of complex **2** is boiled in xylene for 3 h a deep blue solution results from which blue crystals are obtainable¹¹ in 25% yield. Surprisingly this complex has the same chemical composition¹² as **2** and is therefore the third isomer^{13,14} of **2**. The deep blue color is due to an intense absorption band in the red (in benzene solution, λ_{\max} 638 nm; ϵ_{\max} 22500). Proton NMR data¹⁵ are in agreement with the structure **4** for the blue complex. This complex, unlike **2** but true to its phenolic nature, dissolves in aqueous alkali, giving a blue solution. The blue complex has also been examined X-ray crystallographically.¹⁶ Unfortunately there is the complication of crystallographic disorder. The crystal consists of discrete mononuclear molecules. The central platinum atom resides on a site of *mm* symmetry and the ligands are disordered. The Pt–N and C–O(H) distances are respectively 1.962 (6) and 1.29 (3) Å. The five-membered chelate rings and the platinum coordination sphere are planar. The O(H)⋯NNPt distance of 2.60 (3) Å is indicative of hydrogen bonding, which may be responsible for the broadness of the OH proton NMR signal.¹⁵ In the reaction **2** → **4** an oximato oxygen may be utilized to hydroxylate an adjacent aromatic ring, although proof of an intramolecular redox transformation is lacking at present. The blue color of 'platinum blues' is usually associated with a polynuclear mixed-valence core.¹⁷ The present work shows that a

(7) AgClO₄ or AgNO₃ can be used. We have now found that the presence of Ag⁺ ion is not essential for the reaction **1** → **3**. The same result is achieved though very slowly simply by boiling **1** in water. Addition of 1 mol of OH⁻ hastens the reaction very considerably.

(8) The solid is extracted with dichloromethane followed by chromatography of the extract on silica gel using benzene as the eluant. Anal. Calcd for C₁₂H₁₀N₃OClPd: C, 40.71; H, 2.85; N, 11.87. Found: C, 40.80; H, 3.09; N, 11.55.

(9) Crystal data for PdC₁₂H₁₀N₃OCl: triclinic, *P*1̄; *a* = 8.950 (2) Å, *b* = 9.867 (3) Å, *c* = 7.291 (2) Å, α = 105.85 (3)°, β = 96.36 (3)°, γ = 80.06 (3)°, *V* = 608.7 (3) Å³, *Z* = 2, d_{calcd} = 1.93 g/cm³; μ (Mo K α) = 17.0 cm⁻¹. An automated diffractometer (Enraf-Nonius CAD-4) was used to gather 2070 data with $F_o^2 \geq 3\sigma(F_o^2)$. The structure was solved by direct methods and refined to residuals of *R* = 0.0407 and *R_w* = 0.0484 and a quality of fit index of 1.194. $R = \sum ||F_o| - |F_c|| / \sum |F_o|$; $R_w = [\sum w(|F_o| - |F_c|)^2 / \sum w|F_o|^2]^{1/2}$, $w = 1/\sigma^2(F_o)$; quality of fit = $[\sum w(|F_o| - |F_c|)^2 / (N_{\text{obsd}} - N_{\text{parameters}})]^{1/2}$.

(10) In the reaction **1** → **3**, hydroxylation could have occurred at C(7) rather than at C(11) (Figure 1). Proton NMR data on bulk samples however show that only a single species (CH₃ signal at 2.06 ppm in CD₂Cl₂) is present.

(11) The reaction mixture is evaporated to dryness, and the mass is extracted with benzene. The benzene extract is purified by chromatography on silica gel using benzene as the eluant.

(12) Anal. Calcd for PtC₁₆H₁₆N₆O₂: C, 36.99; H, 3.10; N, 16.18. Found: C, 37.16; H, 3.27; N, 16.01.

(13) The second isomer of **2** is the corresponding cis isomer the structure of which is accurately known.¹⁴

(14) Bandyopadhyay, D.; Bandyopadhyay, P.; Chakravorty, A.; Cotton, F. A.; Falvello, L. R. *Inorg. Chem.* **1983**, *22*, 1315.

(15) Two equally intense methyl signals (in CD₂Cl₂ at 200 MHz) occur at 2.50 and 2.54 ppm. That these two signals do not arise from spin-spin coupling was established by parallel experiments at 90 MHz. The aromatic region is highly structured and covers the range 6.9–7.8 ppm. The signals at relatively high field (6.9–7.2 ppm) are assignable to protons of the phenolic ring. The broad OH proton signal occurs at 11 ppm and vanishes upon shaking the solution with D₂O. The intensity ratios of the methyl, aromatic, and phenolic regions are correct for **4**.

(16) Crystal data for blue PtC₁₆H₁₆N₆O₂: Orthorhombic, space group *Pnmm*; *a* = 3.595 (1) Å, *b* = 12.982 (2) Å, *c* = 18.008 (3) Å; *V* = 840.3 (3) Å³; d_{calcd} = 2.052 g/cm³; μ (Mo K α) = 88.1 cm⁻¹. Intensity data (742 reflections with $F_o^2 \geq 3\sigma(F_o^2)$) were gathered by an Enraf-Nonius CAD-4 diffractometer. The structure was solved by Patterson methods and refined to *R* = 0.0374, *R_w* = 0.0431, quality of fit = 1.085; *R*, *R_w*, and quality of fit defined as in ref 9.

(17) Lippard, S. J. *Science (Washington, D.C.)* **1982**, *218*, 1075.

deep blue color in platinum complexes can arise for different reasons^{18,19} in different cases.

Reactions of type **1** → **3** also occur when substituents in the phenyl ring are changed. We are examining the general applicability of this type of hydroxylation reaction in other palladium complexes having pendant phenyl rings close to a reactive bond (e.g. PdCl). The reaction **2** → **4** is only one example of a type of hydroxylation that also occurs in related molecules, e.g., where the ring substituent is C₆H₅ rather than CH₃. This entire class of (presumably intramolecular) redox transformations in metal complexes of oximes is under active study.

Acknowledgment. We are indebted to the Department of Science and Technology, New Delhi, India, and The Robert A. Welch Foundation (Grant A-494) for financial support.

Supplementary Material Available: Tables of atomic parameters, bond lengths and angles, and observed and calculated structure factors for complex **3** (18 pages). Ordering information is given on any current masthead page.

(18) Overbosch, P.; van Koten, G.; Grove, D. M.; Spek, A. L.; Duisenberg, A.J.M. *Inorg. Chem.* **1982**, *21*, 3253.

(19) In our blue complex the color is undoubtedly due to charge-transfer transitions involving both ligand and metal orbitals.

(20) **Note Added in Proof:** The structure of **1** has now been accurately determined.

Mechanism of an Oscillating Organic Reaction: Oxidation of Benzaldehyde with O₂ Catalyzed by Co/Br

Mark G. Roelofs,^{*1a} E. Wasserman,^{*1a} James H. Jensen,^{1b}
and Allan E. Nader^{1c}

E. I. du Pont de Nemours & Company, Inc.
Experimental Station
Wilmington, Delaware 19898
Received May 26, 1983

The O₂ oxidation of benzaldehyde to benzoic acid, catalyzed by Co²⁺/Br⁻, was recently discovered to exhibit sustained oscillations.² Coincident variations in solution color and electrode potential were observed. We describe here the time dependence of dissolved oxygen, [Co³⁺], and PhCHO concentrations and suggest a mechanism to account for the oscillations. The mechanism postulates that in one stage of the reaction benzoyl radical reacts primarily with oxygen, while in the second, benzoyl is oxidized by Co³⁺.

During stage I, the potential of the Pt electrode rises slowly and approximately linearly with the time until it reaches a maximum (Figure 1). (Note that the conditions are different in Figures 1a, 1b, and 2 to highlight pertinent features.) In stage II, the potential abruptly decreases to a minimum. At the maximum, the color of the solution is the dark green characteristic of Co³⁺ in acetic acid.^{3,4} At the potential minimum, the solution exhibits the pale pink color of Co²⁺ in acetic acid. Under typical conditions (see caption, Figure 1), the amplitude of the oscillations is 50–80 mV with a period of 50–400 s.

The log [Co³⁺] parallels the potential in Figure 1a. Furthermore, [Co³⁺] increases approximately exponentially during stage I, indicating an autocatalytic production of Co³⁺. Under some conditions, the maximum [Co³⁺] is less than 5% of the total amount of cobalt, and therefore, depletion of Co²⁺ is not required for oscillations.

(1) (a) Central Research and Development Department. (b) Biochemicals Department. (c) Petrochemicals Department.

(2) Jensen, J. H. *J. Am. Chem. Soc.* **1983**, *105*, 2639–2641.

(3) Jones, G. H. *J. Chem. Res., Synop.* **1981**, 228–229. Jones, G. H. *J. Chem. Res., Miniprint* **1981**, 2801–2868.

(4) Lande, S. S.; Falk, C. D.; Kochi, J. K. *J. Inorg. Nucl. Chem.* **1971**, *33*, 4101–4109.

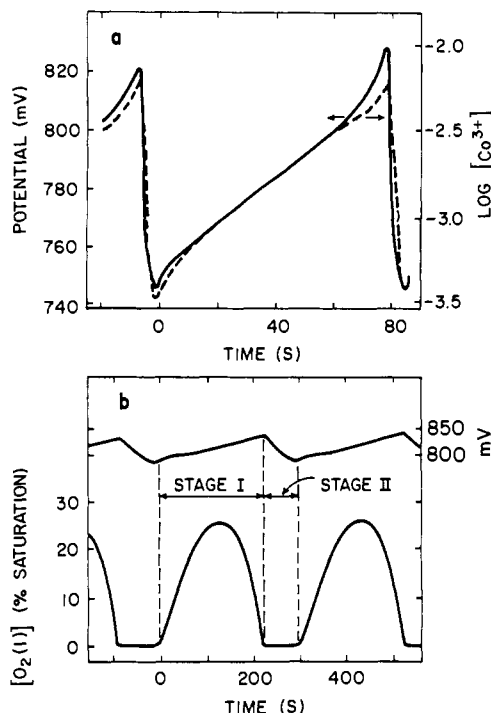


Figure 1. (a) Oscillations of the platinum electrode potential vs. Ag/AgCl reference electrode (—) and log [Co³⁺] determined by optical absorption at 620 nm (---). A 150-mL solution contained initially 500 nM PhCHO, 10 mM Co(AcO)₂, 5 mM NaBr, and 90/10 w/w AcOH/H₂O as solvent. The temperature was 70 °C, an O₂ pressure of 580 torr was maintained above the solution, and the magnetic stirring speed was 400 rpm. (b) A comparison of the Pt electrode response (top trace) with the dissolved oxygen concentration (bottom trace) expressed in terms of the percentage of saturation with O₂ at a partial pressure of 580 torr. We estimate that 100% on this scale corresponds to [O₂(l)] = 5 ± 2 mM. Conditions are as in (a), but the solution contained initially 750 mM PhCHO, 20 mM Co(AcO)₂, and 2 mM NaBr; O₂ was introduced at a flow rate of 20 mL/min through a frit immersed in the liquid.

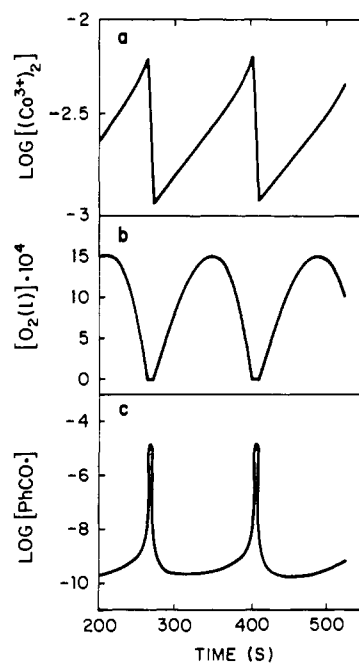


Figure 2. Calculated concentration oscillations in (a) [(Co³⁺)₂], (b) [O₂(l)], and (c) [PhCO].

The dissolved oxygen concentration ([O₂(l)]) was followed with a Clark-type oxygen sensor (Altex) (Figure 1b). At the start of stage I, [Co³⁺] is low and [O₂(l)] is less than our detection limit (1% of saturation). Initially, [O₂(l)] rises as does [Co³⁺]. About halfway through stage I, [O₂(l)] begins to fall; i.e., the increasing